Inorganic Chemistry
Article

Inorg. Chem. **2009**, *48*, 7953–7961 **7953**
DOI: 10.1021/ic900997p

Kinetic and Thermodynamic Stability of the Group 13 Trihydrides

Brian Vest,[†] Karl Klinkhammer,[‡] Christian Thierfelder,[†] Matthias Lein,[†] and Peter Schwerdtfeger*[,†]

[†]*Centre for Theoretical Chemistry and Physics (CTCP), New Zealand Institute for Advanced Study (NZIAS), Massey University Albany, Private Bag 102904, North Shore MSC, Auckland, New Zealand, and* [‡]*Institut für Anorganische und Analytische Chemie, Johannes-Gutenberg-Universität Mainz, Duesbergweg 10-14, D-55128 Mainz, Germany*

Received May 21, 2009

The kinetic and thermodynamic stabilities of the group 13 hydrides EH_3 (E = B, Al, Ga, In, Tl, E113) are investigated by relativistic density functional and wave function based theories. The unimolecular decomposition of $EH_3 \rightarrow EH + H_2$ becomes energetically more favorable going down the Group 13 elements, with the H_2-abstraction of InH_3, TlH_3, and $(E113)H_3$ (E113: element with nuclear charge 113) being exothermic. In accordance with the Hammond−Leffler postulate, the activation barrier for the dissociation process decreases accordingly going down the group 13 elements in the periodic table shifting to an early transition state, with activation energies ranging from 88.4 kcal/mol for BH_3 to 41.3 kcal/mol for TlH_3 and only 21.6 kcal/mol for $(E113)H_3$ at the scalar relativistic coupled cluster level of theory. For both TlH_3 and $(E113)H_3$ we investigated spin−orbit effects using Dirac−Hartree−Fock and second-order Møller−Plesset theory to account for electron correlation. For (E113)H, spin−orbit coupling results in a chemically inert closed $7p_{1/2}$-shell, thus reducing the stability of the higher oxidation state even further. We also investigated the known organothallium compound $Tl(CH_3)_3$, which is thermodynamically unstable similar to TlH_3, but kinetically very stable with an activation barrier of 57.1 kcal/mol.

Introduction

The stability and chemical properties of the group 13 hydrides EH_3 (E = B, ..., Tl) have been a topic of intense discussion and debate for many decades.[1] More than 60 years ago, Egon Wiberg and co-workers claimed the synthesis and isolation of the group 13 trihydrides EH_3 (E = B−Tl).[2] However, the last confirmed successful synthesis was gallane by Downs et al.[1] who were able to isolate GaH_3 as a white solid which melts at −50 °C. Any other attempts to reproduce Wiberg's results in the synthesis of InH_3 and TlH_3 have been unsuccessful.[3] According to several authors,[4−8] it seems unlikely that InH_3 and TlH_3 are stable enough to be isolated in the solid phase under normal conditions.

Unlike the group 13 monohydrides (EH), whose gas-phase stabilities have allowed them to be studied extensively by spectroscopic methods,[9] the gas-phase stability of the heavier InH_3 and TlH_3 has been problematic as well. Even two more recent review articles listed these compounds as being nonexistent in the gas-phase.[10] Until very recently, only the lighter EH_3 and E_2H_6 (E = B, Al, Ga) have been studied extensively through spectroscopy.[5,11−19] InH_3 and TlH_3 were

*To whom correspondence should be addressed. E-mail: p.a.schwerdtfeger@massey.ac.nz.

(1) Downs, A. J.; Goode, M. J.; Pulham, C. R. *J. Am. Chem. Soc.* **1989**, *111*, 1936.
(2) (a) Wiberg, E.; Johannsen, T. *Naturwissenschaften* **1941**, *29*, 320. (b) Stecher, O.; Wiberg, E. *Ber. Dtsch. Chem. Ges.* **1942**, *75*, 2003. (c) Wiberg, E.; Johannsen, T. *Angew. Chem.* **1942**, *55*, 38. (d) Wiberg, E.; Johannsen, T.; Stecher, O. Z. *Anorg. Allg. Chem.* **1943**, *251*, 114. (e) Wiberg, E.; Schmidt, M. *Z. Naturforsch. B* **1951**, *6*, 171. (f) Wiberg, E.; Schmidt, M. *Z. Naturforsch. B* **1951**, *6*, 172. (g) Wiberg, E.; Schmidt, M. *Z. Naturforsch. B* **1951**, *6*, 334. (h) Wiberg, E.; Schmidt, M. *Z. Naturforsch. B* **1951**, *6*, 335. (i) Wiberg, E.; Schmidt, M. *Z. Naturforsch. B* **1952**, *7*, 577. (j) Wiberg, E.; Dittmann, O. *Z. Naturforsch. B* **1957**, *12*, 57. (k) Wiberg, E.; Dittmann, O.; Nöth, H.; Schmidt, M. *Z. Naturforsch. B* **1957**, *12*, 61.
(3) Taylor, M. J.; Brothers, P. J. *Chemistry of Aluminum, Gallium, Indium, and Thallium*; Downs, A. J., Ed.; Blackie: Glasgow, Scotland, 1993; p. 111.
(4) (a) Shriver, D. F.; Parry, R. W.; Greenwood, N. N.; Storr, A.; Wallbridge, M. G. H. *Inorg. Chem.* **1963**, *2*, 867. (b) Greenwood, N. N.; Wallbridge, M. G. H. *J. Chem. Soc.* **1963**, 3912.
(5) Breisacher, P.; Siegel, B. *J. Am. Chem. Soc.* **1965**, *87*, 4255.
(6) Schwerdtfeger, P. *Phys. Scr.* **1987**, *36*, 453.
(7) Schwerdtfeger, P.; Heath, G. A.; Dolg, M.; Bennett, M. A. *J. Am. Chem. Soc.* **1992**, *114*, 7518.
(8) Hunt, P.; Schwerdtfeger, P. *Inorg. Chem.* **1996**, *35*, 2085.
(9) Huber, K. P.; Herzberg, G. *Constants of Diatomic Molecules*; Van Nostrand-Reinhold: New York, 1979.
(10) (a) Downs, A. J.; Pulham, C. R. *Chem. Soc. Rev.* **1994**, *1994*, 175. (b) Aldridge, S.; Downs, A. J. *Chem. Rev.* **2001**, *101*, 3305.
(11) (a) Rigden, J. S.; Koski, W. S. *J. Am. Chem. Soc.* **1961**, *83*, 3037. (b) Bayliss, A. B.; Pressley, G. A., Jr.; Stafford, F. E. *J. Am. Chem. Soc.* **1966**, *88*, 2428. (c) Fehlner, T. P.; Koski, W. S. *J. Am. Chem. Soc.* **1964**, *86*, 2733. (d) Ruscic, B.; Mayhew, C. A.; Berkowitz, J. *J. Chem. Phys.* **1988**, *88*, 5580.
(12) Kaldor, A.; Porter, R. F. *J. Am. Chem. Soc.* **1971**, *93*, 2140.
(13) Kawaguchi, K.; Butler, J. E.; Yamada, C.; Bauer, S. H.; Minowa, T.; Kanamori, H.; Hirota, E. *J. Chem. Phys.* **1987**, *5*, 2438.
(14) Kurth, F. A.; Eberlein, R. A.; Schnöckel, H.; Downs, A. J.; Pulham, C. R. *J. Chem. Soc., Chem. Commun.* **1993**, 1302.
(15) Chertihin, G. V.; Andrews, L. *J. Phys. Chem.* **1993**, *97*, 10295.
(16) Andrews, L.; Wang, X. *J. Phys. Chem. A* **2004**, *108*, 4202.

Published on Web 07/14/2009

only recently synthesized in the gas phase, with TlH_3 being produced through laser-ablation matrix-isolation spectroscopy within hydrogen or inert gas matrixes at cryogenic temperatures.[19−22]

Similar to trihydrides of the group 13 elements, the trialkyl and triaryl compounds of thallium, for example, $TlMe_3$ (Me = CH_3), have also been shown to be unstable in the gas phase.[23] In contrast, the trimethyl derivatives of the lighter group 13 compounds are all thermodynamically stable species.[24] The organothallium compounds are however kinetically stable and can be isolated in solid form.[25] Unlike the monohydrides, the monoalkyls of Tl(I) have never been isolated, with one notable exception by Uhl and co-workers, who in 1997 synthesized for the first time $Tl[C(SiMe_3)_3]$.[26] In the solid state this compound adopts an unusual distorted tetrahedral structure consisting of Tl atoms forming weak Tl−Tl bonds. In 1998 Niemeyer and Power reported the synthesis of the first well characterized thallium monoaryl employing the very bulky terphenyl substituent 2,6-$Trip_2C_6H_3$ (Trip = 1,3,5- iPr$_3$C$_6$H$_2$). It is a monomer even in the solid state and comprises a singly coordinated thallium atom.[27] Reducing the sterical congestion of the terphenyl group allowed for the isolation of further thallium(I) aryls which dimerize or trimerize in the solid state via weak Tl−Tl interactions.[28] We mention that both cyclopentadienyl-Tl(I) and -In(I) compounds are well-known.[29] Most notably Schumann and co-workers synthesized (η^5-pentabenzyl-cyclopentadienyl)-thallium(I) in dimeric form in the solid state with relatively short Tl−Tl distances.[30] The strength of such Tl−Tl interactions have been the subject of some debate.[31] A comprehensive review on organothallium(I) and (II) chemistry has been given by Janiak.[32] The only other monoalkyls of thallium are Tl(III) compounds of the type $RTlX_2$ and RTlO (X = OAc, CN, Cl, Br, ...).[24,33]

It is well-known that the stability of the group 13 compounds MX_3 (X any ligand) decreases going down the periodic table, as the highest oxidation state becomes increasingly more unstable.[7,34,35] Schwerdtfeger et al. have shown that the decomposition of TlH_3 to TlH and H_2 is an exothermic process,[6] with InH_3 being borderline.[7] They further demonstrated that the decomposition of the lighter EH_3 compounds is likely to be thermodynamically unfavorable. The reason for the instability of the higher oxidation states of the post-lanthanide elements has been debated for many years.[7,8,36−38] Hence, several theories have arisen in an attempt to explain the low valency nature of these elements. The primary theory used to explain this phenomenon, developed by Sidgwick,[36] is called the "inert pair effect", which is attributed to the apparent inertness of the 6s electrons. This theory has later been criticized based on two important points. If the 6s electron pair is particularly inert, then there should be a large increase in the 6s ionization potential going from In to Tl, which is not the case.[39] Also, the $6s^2 \rightarrow 6s^16p^1$ energy gap for Tl^+ is not unusually large and comparable to that of Ga^+.[39] Drago[38] analyzed the inert pair effect for the chlorides of groups 13 and 14 and concluded that the low-valencies are attributed to the decrease in the covalent contribution to the metal-chlorine bond for the heavier elements. Schwerdtfeger et al.[7] also came to the same conclusion for the group 13 hydrides and halides. They further demonstrated that the instability of EH_3 is not attributed to an increase in the metal-hydride bond strength in EH, rather the breaking of the progressively weaker E−H bonds of the heavier hydrides and the concomitant formation of a strong H−H bond led to favorable decomposition of the heavier hydrides.[7]

Relativistic effects also play an important role in determining the properties of the heavier EH and EH_3 molecules. The inclusion of scalar relativistic pseudopotentials has been shown to decrease the metal−hydrogen bond length of TlH and TlH_3 significantly.[6,7] More importantly, the dipole moments of TlH and in the eka-thallium (the element with nuclear charge 113 abbreviated as E113 for the following) compound (E113)H increased greatly with the inclusion of scalar relativistic effects, despite the decrease in bond length.[40] The spin−orbit (SO) splitting of the $np^{1/2}$ and $np^{3/2}$ orbitals in Tl and E113 is already non-negligible (0.97 and 2.79 eV, respectively for the $^2P_{1/2}/^2P_{3/2}$ splitting).[39,41] The inclusion of spin−orbit effects has also been shown to greatly influence the Tl−H and (E113)−H bond lengths.[7,42,43] Interestingly, the minimum geometry of $(E113)H_3$ was calculated to be T-shaped (C_{2v} symmetry) and not trigonal planar

(17) Hara, M.; Domen, K.; Onishi, T.; Nozoye, H. *J. Phys. Chem.* **1991**, *95*, 6.
(18) Wang, X.; Andrews, L. *J. Phys. Chem. A* **2003**, *107*, 11371.
(19) Pullumbi, P.; Bouteiller, Y.; Manceron, L.; Mijoule, C. *Chem. Phys.* **1994**, *185*, 25.
(20) Andrews, L.; Wang, X. *Angew. Chem., Int. Ed.* **2004**, *43*, 1706.
(21) Wang, X.; Andrews, L. *J. Phys. Chem. A* **2004**, *108*, 4440.
(22) Wang, X.; Andrews, L. *J. Phys. Chem. A* **2004**, *108*, 3396.
(23) (a) Gilman, H.; Jones, R. G. *J. Am. Chem. Soc.* **1946**, *68*, 517. (b) Gilman, H.; Jones, R. G. *J. Am. Chem. Soc.* **1950**, *72*, 1760. (c) Canty, A. J.; Colton, R.; Thomas, I. M. *J. Organomet. Chem.* **1993**, *455*, 283.
(24) Coates, G. E.; Green, M. L. H.; Wade, K. *Organometallic Compounds*; Methuen & Co., Ltd.: London, 1982.
(25) (a) Sheldrick, G. M.; Sheldrick, W. S. *J. Chem. Soc. A* **1970**, 28. (b) Boese, R.; Downs, A. J.; Greene, T. M.; Hall, A. W.; Morrison, C. A.; Parsons, S. *Organomet.* **2003**, *22*, 2450.
(26) Uhl, W.; Keimling, S. U.; Klinkhammer, K. W.; Schwarz, W. *Angew. Chem., Int. Ed.* **1997**, *36*, 64.
(27) Niemeyer, M.; Power, P. P. *Angew. Chem., Int. Ed.* **1998**, *37*, 1277.
(28) Wright, R. J.; Phillips, A. D.; Hino, S.; Power, P. P. *J. Am. Chem. Soc.* **2005**, *127*, 4799.
(29) (a) Fischer, E. O. *Angew. Chem.* **1957**, *69*, 207. (b) Cotton, F. A.; Reynolds, L. T. *J. Am. Chem. Soc.* **1958**, *80*, 269.
(30) Schumann, H.; Janiak, C.; Pickardt, J.; Börner, U. *Angew. Chem., Int. Ed. Engl.* **1987**, *26*, 789.
(31) (a) Janiak, C.; Hoffmann, R. *Angew. Chem., Int. Ed. Engl.* **1989**, *28*, 1688. (b) Janiak, C.; Hoffmann, R. *J. Am. Chem. Soc.* **1990**, *112*, 5924. (c) Schwerdtfeger, P. *Inorg. Chem.* **1991**, *30*, 1660.
(32) Janiak, C. *Coord. Chem. Rev.* **1997**, *163*, 107.
(33) (a) Lee, A. G. *The Chemistry of Thallium*; Elsevier: Amsterdam, The Netherlands, 1971; (b) Abel, E. W.; Stone, F. G. A. *Organometallic Chemistry*; The Royal Society of Chemistry: London, 1971−1987; Vol. *I-XV*. (c) Buckingham, J.; MacIntyre, J. *Dictionary of Organometallic Compounds*; Chapman & Hall: London, 1982.
(34) Schwerdtfeger, P.; Boyd, P. D. W.; Bowmaker, G. A.; Mack, H. G.; Oberhammer, H. *J. Am. Chem. Soc.* **1989**, *111*, 15.
(35) (a) Schwerdtfeger, P.; Ischtwan, J. *J. Comput. Chem.* **1993**, *14*, 913. (b) Schwerdtfeger, P.; Ischtwan, J. *J. Molec. Stuct., THEOCHEM* **1994**, *306*, 9.
(36) (a) Sidgwick, N. V. *Some Physical Properties of the Covalent Link in Chemistry*; Cornell University Press: Ithaca, NY, 1933; pp 189 and 210. (b) Sidgwick, N. V. *Ann. Rep.* **1933**, *30*, 120. (c) Sidgwick, N. V. *The Chemical Elements and their Compounds*; Clarendon Press: Oxford, 1950; Vol. *1*, p 287.
(37) (a) Grimm, H. G. *Z. Phys.* **1921**, *98*, 353. (b) Stoner, E. C. *Philos. Mag.* **1924**, *48*, 719. (c) Grimm, H. G.; Sommerfeld, A. *Z. Phys.* **1926**, *36*, 36.
(38) Drago, R. S. *J. Phys. Chem.* **1958**, *62*, 353.
(39) Moore, C. E. *Atomic Energy Levels*; Natl. Bur. Stand. (U.S.) Circ. No. 467; U.S. GPO: Washington D.C., 1958.
(40) Liu, W.; Wüllen, C.; Wang, F.; Li, L. *J. Chem. Phys.* **2002**, *116*, 3626.
(41) Eliav, E.; Kaldor, U.; Ishikawa, Y.; Seth, M.; Pyykkö, P. *Phys. Rev. A* **1996**, *53*, 3926.
(42) Han, Y.-K.; Bae, C.; Lee, Y. S. *J. Chem. Phys.* **1999**, *110*, 9353.
(43) Seth, M.; Schwerdtfeger, P.; Faegri, K. *J. Chem. Phys.* **1999**, *111*, 6422.

(D_{3h} symmetry) like all the other group 13 trihydrides, which is due to the large relativistic contraction of the 7s orbital and relativistic 6d expansion allowing for additional 6d-7s mixing in the metal−hydrogen bond.[43] We note that relativistic effects in thallium(I)−carbon force constants such as $TlMe_2^+$ can be unexpectedly large according to a theoretical study,[44] explaining the observed anomaly of the metal−carbon bond-strength in the series of MMe_2 compounds of the heavy elements with M = Au^-, Hg, Tl^+, and Pb^{2+}.[45]

Although the energies of the decomposition of group 13 trihydrides EH_3 have been studied extensively, there appears to be no study on examining the kinetics or the mechanism of the decomposition process. We mention, however, that Merino et al.[46] have undertaken theoretical calculations on the mechanism for the decomposition of the group 14 tetrahydrides, while the thermodynamics and relativistic effects in the decomposition was studied earlier by Seth et al.[48] Merino et al. have shown that the decomposition of these compounds involves a two-step process, in which the original T_d symmetry was broken with the formation of a bond between two of the hydrogens, leading to a product of C_s symmetry. These product structures were high-lying local minima for Si, Ge, and Sn but low-lying for Pb, and they consisted primarily of a hydrogen molecule weakly bound to the EH_2 product. In a recent paper van Stralen and Bickelhaupt studied the oxidative addition versus dehydrogenation of the Group 14 tetrahydrides reacting with palladium using the zero-order relativistic approximation within density functional theory.[47] They found the dehydrogenation enthalpies decreasing down the Group 14 hydrides with the decomposition of PbH_4 being exothermic in agreement with previous studies.[48] Concerning the transition state it is unknown whether the group 13 hydrides decompose in a similar fashion to the Group 14 hydrides. Hence, this paper is primarily focused on determining the unimolecular decomposition pathways of the group 13 hydrides EH_3 from boron to E113 to their corresponding monohydrides with concomitant loss of hydrogen, that is, $EH_3 \rightarrow EH + H_2$. We also include the decomposition of $TlMe_3$ to TlMe and ethane in our study to determine a plausible mechanism for this gas phase decomposition.

Computational Methods

Geometry optimizations were performed using the Gaussian03 program package[49] for all of the EH and EH_3 molecules (E = B to Tl) applying second-order many-body perturbation theory (MP2) and coupled-cluster with single and double substitutions including non-iterative triples (CCSD(T)) within a fully active orbital space, and density functional theory (DFT) using Becke's hybrid functional B3LYP,[50] and the gradient corrected functional PW91[51] with augmented correlation consistent triple-ζ basis sets (aug-cc-pVTZ) for boron and aluminum.[52] For gallium, indium, and thallium, we used augmented weighted-core basis sets of triple-ζ quality (aug-cc-pwCVTZ).[53] Thus, for the gallium, indium, and thallium compounds the correlation space includes the lower lying core n(spd) orbitals. For the larger molecule $TlMe_3$, geometry optimizations were performed using MP2 with a fully active orbital space together with an aug-cc-pwCVTZ basis set for Tl[53] and aug-cc-pVTZ basis sets for C and H.[52] At the optimized MP2 geometries (minima and transition state), we performed single-point CCSD(T) calculations for the decomposition of $TlMe_3$ into TlMe + C_2H_6. Relativistic effects were accounted for through the use of energy-consistent scalar-relativistic small-core pseudopotentials for Ga, In, and Tl.[54] For E113, we applied the scalar relativistic pseudopotential and corresponding valence basis set as published earlier by Seth et al.[43]

Harmonic frequency analyses were performed on the optimized structures to determine if they represent minima or transition states, as well as to obtain zero-point vibrational energies, enthalpies, Gibbs free energies, and entropies of the various species. Intrinsic reaction coordinate (IRC) calculations[55] were performed at the MP2 level of theory to obtain energy profiles in both the forward and reverse directions, and to ascertain that the transition state connects to the correct starting and ending points on the potential energy surface. For the IRC calculations, we used a maximum of 50 steps in both the forward and the reverse directions with a step size of 0.1 $amu^{1/2}$ Bohr. For $TlMe_3$, we used a maximum of 25 steps in both directions with a step size of 0.2 $amu^{1/2}$ Bohr, as these computations were very computer time-consuming. To calculate the weakly bound product between EH and H_2, we used the last point in the IRC analysis and reoptimized their structures at the MP2 level of theory. Anharmonic corrections to the vibrational modes of EH_3 were also calculated. The perturbative approach used here is described in detail by Schaefer and co-workers[56] as implemented in Gaussian03[49] by Barone and co-workers.[57]

(44) Schwerdtfeger, P. *J. Am. Chem. Soc.* **1990**, *112*, 2818.
(45) (a) Hobbs, Ch. W.; Tobias, S. *Inorg. Chem.* **1970**, *9*, 1998. (b) Miles, M. G.; Patterson, J. H.; Hobbs, C. W.; Hopper, M. J.; Overend, J.; Tobias, R. S. *Inorg. Chem.* **1968**, *7*, 1721. (c) Freidline, C. E.; Tobias, R. S. *Inorg. Chem.* **1966**, *5*, 354. (d) Adams, D. M. In *Metal-Ligand and Related Vibrations*; Edward Arnold: London, 1967; p 206.
(46) Merino, G.; Escalante, S.; Vela, A. *J. Phys. Chem. A* **2004**, *108*, 4909.
(47) van Stralen, J. N. P.; Bickelhaupt, F. M. *Organometallics* **2006**, *25*, 4260.
(48) Seth, M.; Faegri, K.; Schwerdtfeger, P. *Angew. Chem., Int. Ed.* **1998**, *37*, 2493.
(49) Frisch, M. J.; Trucks, G. W.; Schlegel, H. B.; Scuseria, G. E.; Robb, M. A.; Cheeseman, J. R.; Montgomery, J. A., Jr.; Vreven, T.; Kudin, K. N.; Burant, J. C.; Millam, J. M.; Iyengar, S. S.; Tomasi, J.; Barone, V.; Mennucci, B.; Cossi, M.; Scalmani, G.; Rega, N.; Petersson, G. A.; Nakatsuji, H.; Hada, M.; Ehara, M.; Toyota, K.; Fukuda, R.; Hasegawa, J.; Ishida, M.; Nakajima, T.; Honda, Y.; Kitao, O.; Nakai, H.; Klene, M.; Li, X.; Knox, J. E.; Hratchian, H. P.; Cross, J. B.; Bakken, V.; Adamo, C.; Jaramillo, J.; Gomperts, R.; Stratmann, R. E.; Yazyev, O.; Austin, A. J.; Cammi, R.; Pomelli, C.; Ochterski, J. W.; Ayala, P. Y.; Morokuma, K.; Voth, G. A.; Salvador, P.; Dannenberg, J. J.; Zakrzewski, V. G.; Dapprich, S.; Daniels, A. D.; Strain, M. C.; Farkas, O.; Malick, D. K.; Rabuck, A. D.; Raghavachari, K.; Foresman, J. B.; Ortiz, J. V.; Cui, Q.; Baboul, A. G.; Clifford, S.; Cioslowski, J.; Stefanov, B. B.; Liu, G.; Liashenko, A.; Piskorz, P.; Komaromi, I.; Martin, R. L.; Fox, D. J.; Keith, T.; Al-Laham, M. A.; Peng, C. Y.; Nanayakkara, A.; Challacombe, M.; Gill, P. M. W.; Johnson, B.; Chen, W.; Wong, M. W.; Gonzalez, C.; Pople, J. A. *Gaussian 03*, Revision C.03; Gaussian, Inc.: Wallingford, CT, 2004.
(50) (a) Vosko, S. H.; Wilk, L.; Nusair, M. *Can. J. Phys.* **1980**, *58*, 1200. (b) Lee, C.; Yang, W.; Parr, R. G. *Phys. Rev. B* **1988**, *37*, 785. (c) Becke, A. D. *J. Chem. Phys.* **1993**, *98*, 5648. (d) Stephens, P. J.; Devlin, F. J.; Chabalowski, C. F.; Frisch, M. J. *J. Phys. Chem.* **1994**, *98*, 11623.
(51) Perdew, J. P.; Chevary, J. A.; Vosko, S. H.; Jackson, K. A.; Pederson, M. R.; Singh, D. J.; Fiolhais, C. *Phys. Rev. B* **1992**, *46*, 6671.
(52) (a) Dunning, T. H., Jr. *J. Chem. Phys.* **1989**, *90*, 1007. (b) Woon, D. E.; Dunning, T. H., Jr. *J. Chem. Phys.* **1993**, *98*, 1358. (c) Kendall, R. A.; Dunning, T. H., Jr.; Harrison, R. J. *J. Chem. Phys.* **1992**, *96*, 6796.
(53) Peterson, K. A.; Yousaf, K., in preparation.
(54) (a) Metz, B.; Stoll, H.; Dolg, M. *J. Chem. Phys.* **2000**, *113*, 2563. (b) Metz, B.; Schweizer, M.; Stoll, H.; Dolg, M.; Liu, W. *Theor. Chem. Acc.* **2000**, *104*, 22.
(55) (a) Gonzalez, C.; Schlegel, H. B. *J. Chem. Phys.* **1989**, *90*, 2154. (b) Gonzalez, C.; Schlegel, H. B. *J. Phys. Chem.* **1990**, *94*, 5523.
(56) Clabo, A. A., Jr.; Allen, W. D.; Remington, R. B.; Yamaguchi, Y.; Schaefer, H. F., III *Chem. Phys.* **1988**, *123*, 187.
(57) (a) Barone, V. *J. Chem. Phys.* **2004**, *120*, 3059. (b) Carbonniere, P.; Lucca, T.; Pouchan, C.; Rega, N.; Barone, V. *J. Comput. Chem.* **2005**, *26*, 384. (c) Barone, V. *J. Chem. Phys.* **2005**, *122*, 014108.

Table 1. Calculated Equilibrium Bond Distances (in Å) for the Group 13 Hydrides EH and EH_3 (E = B to E113) at Various Levels of Theory

method	B	Al	Ga	In	Tl	E113
			Monohydrides EH			
B3LYP	1.232	1.665	1.686	1.860	1.916	1.955
PW91	1.248	1.679	1.694	1.866	1.922	1.958
MP2[a]	1.216	1.644	1.644	1.819	1.872	1.906
CCSD(T)	1.223	1.650	1.660	1.836	1.891	1.931
Exp.[b]	1.232	1.648	1.663	1.838	1.870	-
			Trihydrides EH_3			
B3LYP	1.188	1.582	1.559	1.728	1.745	1.758
PW91	1.196	1.594	1.564	1.731	1.750	1.767
MP2[c,d]	1.181	1.574	1.530	1.692	1.697	1.831/1.635[c,e]
CCSD(T)	1.185	1.580	1.546	1.713	1.723	1.852/1.652[c,f]

[a] At the Dirac-MP2 level of theory the bond distance is 1.847 Å for TlH and 1.703 Å for (E113)H. [b] Experimental values from ref 9. [c] The structures are of C_{2v}symmetry with one long axial bond distance r_a(E113−H_1) and two short equatorial bond distances r_e(E113−$H_{2,3}$). [d] At the Dirac-MP2 level of theory the bond distances are 1.703 Å for TlH_3, and r_a = 1.772 Å and r_e = 1.632 Å for (E113)H with a bond angle of 101.2° between the axial and equatorial bonds. [e] Bond angles of 98.4° between the axial and equatorial bonds. [f] Bond angles of 99.4° between the axial and equatorial bonds.

For the hydrides of thallium and element 113, spin-obit effects cannot be neglected anymore. Hence we performed four-component all-electron Dirac−Hartree−Fock (DHF) calculations followed by MP2 at the optimized scalar relativistic geometries. Here we used Faegri's four component basis sets for Tl and element 113[58] within the program system DIRAC.[59] Variational stability in all four-component calculations was ensured by using dual basis sets[58] with the appropriate kinetic balance condition.[60] In all DFC calculations the (SS|SS) two-electron integrals between the small components were omitted and the Visscher Coulomb correction was applied instead.[61] A Gaussian charge distribution for the finite-size nuclear model was chosen.[62]

Results and Discussion

Properties. The optimized structural parameters for the group 13 hydrides EH and EH_3 are listed in Table 1. We note that the EH_3 molecules are of $^1A_1'$ (D_{3h}) symmetry, and the ground states of EH are of $^1\Sigma^+$ symmetry.[7,63] (E113)H_3 is an exception to this, as both our MP2 and CCSD(T) calculations show that the D_{3h} structure represents a second-order saddle point, and the minimum structure is a symmetry broken $^1A_1$ state of C_{2v} (T-shaped) symmetry with one long axial and two short equatorial bonds, in agreement with previous calculations by Seth et al.[43] However, density functional calculations incorrectly predict the trigonal planar D_{3h} structure as a minimum. It has been pointed out that many density functionals have difficulties in describing correctly second-order Jahn−Teller effects, which requires a correct description of the interacting frontier symmetry-orbitals,[64] that is, AtF_3 and (E117)F_3 represent such difficult cases where density functionals incorrectly describe these symmetry broken structures.[64,65]

Our calculated group 13 element-hydrogen bond lengths are in very good agreement with the available experimental[9] or previously published computational data.[7,8,19,40,43,63,66,67] For example, if we correct our scalar relativistic CCSD(T) bond distance of 1.891 Å in TlH by spin−orbit effects obtained from Dirac-MP2 calculations, we get 1.867 Å in perfect agreement with the experimental value of 1.870 Å.[9] Our spin−orbit corrected CCSD(T) value for the bond distance in (E113)H is 1.728 Å and somewhat shorter than the Dirac-CCSD(T) value previously published by Seth et al. who predict 1.789 Å.[43] Other CCSD(T) calculations by Lee and co-workers gave 1.762 Å using spin−orbit relativistic pseudopotentials.[68] Concerning the trihydrides EH_3, previous coupled cluster calculations[19,63,67] gave bond lengths of 1.187 Å for BH_3[67] (exp. 1.187 Å),[69] 1.586 Å for AlH_3,[19] 1.567 Å for GaH_3,[19] and 1.753 Å for InH_3.[19] Previous scalar relativistic MP2 calculations on TlH_3 gave a Tl−H bond distance of 1.728 Å,[8] and Seth et al.[43] calculated for (E113)H_3 r_a = 1.798 Å, r_e = 1.621 Å, and an angle between the axial and equatorial bonds of 98.6° at the relativistic MP2 level of theory. In comparison, in almost all cases B3LYP and PW91 produce bond lengths which are longer than our CCSD(T) and MP2 values.

The overall trend is that the E−H bond becomes weaker with increasing atomic radius going down the period,[7,9,35] with a subsequent increase in the E−H bond lengths. The exception being the (E113)−H bond distances as spin−orbit effects play an important role in these superheavy element compounds. Here the large spin−orbit splitting between the $7p_{1/2}$ and $7p_{3/2}$ level with a subsequent contraction of the $7p_{1/2}$ orbital compared to the scalar relativistic 7p orbital leads to a shorter (E113)−H distance compared to Tl−H as has been pointed out before.[43] Similar effects are seen for the equatorial bond distance in (E113)H_3. Interestingly, the bond angles for (E113)H_3 are not greatly affected by the inclusion of spin−orbit effects, see Table 1.

For TlMe and ethane, we calculate Tl−C and C−C bond lengths of 2.297 Å and 1.518 Å, respectively, at the MP2 level of theory. The Tl−C−H angle is 110.4°. $TlMe_3$ adopts a trigonal planar C_{3h} geometry, in agreement with earlier gas-phase electron diffraction experiments[70] and quantum-chemical investigations.[34] Here we obtain the following MP2 bond distances (in Å) and angles (in degrees): Tl−C 2.181, C−H(*ip*) 1.084, C−H(*oop*) 1.086,

(58) Faegri, K.; Saue, T. *J. Chem. Phys.* **2001**, *115*, 2456.
(59) DIRAC, a relativistic ab initio electronic structure program, Release 3.1, written by Saue, T.; Enevoldsen, T.; Helgaker, T.; Jensen, H. J. Aa.; Laerdahl, J. K.; Ruud, K.; Thyssen, J.; Visscher, L. See http://dirac.chem.sdu.dk; Saue, T.; Fægri, K., Jr.; Helgaker, T.; Gropen, O. *Mol. Phys.* **1997**, *91*, 937.
(60) Dyall, K. G.; Faegri, K., Jr. *Chem. Phys. Lett.* **1990**, *174*, 25.
(61) Visscher, L.; Aerts, P. J. C.; Visser, O.; Nieuwpoort, W. C. *Int. J. Quantum Chem. Symp.* **1991**, *25*, 131.
(62) Visscher, L.; Dyall, K. G. *At. Data Nucl. Data Tables* **1997**, *67*, 207.
(63) Bartmess, J. E.; Hind, R. J. *Can. J. Chem.* **2005**, *83*, 2005.
(64) Schwerdtfeger, P. *J. Phys. Chem.* **1996**, *100*, 2968.
(65) Kim, H.; Choi, Y. J.; Lee, Y. S. *J. Phys. Chem.* **2008**, *112*, 16021.
(66) (a) Pople, J. A.; Luke, B. T.; Frisch, M. J.; Binkley, J. S. *J. Chem. Phys.* **1985**, *89*, 2198. (b) Treboux, G.; Barthelat, J.-C. *J. Am. Chem. Soc.* **1993**, *115*, 4870.
(67) Schuurman, M. S.; Allen, W. D.; Schaefer, H. F., III *J. Comput. Chem.* **2005**, *26*, 1106.
(68) Han, Y.-K.; Bae, C.; Son, S.-K.; Lee, Y. S. *J. Chem. Phys.* **2000**, *112*, 2684. (b) Choi, Y. J.; Han, Y.-K.; Lee, Y. S. *J. Chem. Phys.* **2001**, *115*, 3448. (c) Choi, Y. J.; Lee, Y. S. *J. Chem. Phys.* **2003**, *119*, 2014.
(69) Kawaguchi, K. *J. Chem. Phys.* **1992**, *96*, 3411.
(70) Fjeldberg, T.; Haaland, A.; Seip, R.; Shen, Q.; Weidlein, J. *Acta Chem. Scand. A* **1982**, *36*, 495.

Table 2. Calculated Harmonic (H), ω_e, and Fundamental Anharmonic (AH), ν, Vibrational Frequencies (in cm^{-1}) for the Group 13 Hydrides EH (E = B to E113) at the MP2 Level of Theory[a]

molecule	method	ω_e(H)	ν(AH)
BH	MP2	2470 (388)	2370
	IR (gas)[9]	2366.9	2269.2
AlH	MP2	1706 (725)	1648
	MI-IR (H_2/Ar)[15]		1591.4
	MI-IR (Ne)[16]		1610.8
	IR (gas)[9]	1682.6	1625.2
GaH	MP2	1652 (898)	1595
	MI-IR (H2)[18]		1516.9
	IR (gas)[9]	1604.5	1548.2
InH	MP2	1509 (1006)	1459
	MI-IR (H2)[20]		1393.4
	IR (gas)[9]	1476.0	1425.8
TlH	MP2	1420 (1161)	1375
	MI-IR (H_2)[22]		1311.3
	IR (gas)[9]	1390.7	1345.3
(E113)H	MP2	1462 (1009)	1458

[a] The calculated IR intensities (in km/mol) are given within parentheses after the harmonic frequency. For the IR(gas) harmonic and anharmonic frequencies see ref 9 for details.

C−Tl−C 120.0, Tl−C−H(*ip*) 111.1 Tl−C−H(*oop*) 108.7, and torsion angles C−Tl−C−H(*ip*) 0.0, C−Tl−C−H-(*oop*) 59.0 (*ip* denotes in-plane and *oop* out-of-plane). Our calculated Tl−C distance is in good agreement with previous relativistic pseudopotential MP2 calculations which gave 2.152 Å.[34]

The results of our frequency analyses for EH and EH_3 are given in Tables 2 and 3 along with literature data. The vibrational spectrum of trimethylthallium has been investigated by theoretical and experimental methods in detail in the past and will not be repeated here.[71] Our calculated frequencies are in relatively good agreement with the experimental values for all of the EH and EH_3 molecules, especially for the out of plane (ν_2) and in-plane (ν_4) bending modes in EH_3. The stretching frequencies are overestimated at the MP2 level of theory and more accurate coupled cluster calculations are required to reach experimental accuracy. However, some interesting trends among the different vibrational modes are found. The value of the asymmetric stretching mode ν_3 for BH_3 is significantly larger than that for the symmetric one, ν_1. These two frequencies are about the same for AlH_3, and for the heavier trihydrides, the two frequencies are reversed, with ν_3 being smaller than ν_1. As the hydrides become less stable with increasing nuclear charge of the group 13 atom, the asymmetric mode leads toward the decomposition pathway on the potential energy surface (see discussion below), which most likely is already reflected in a lower asymmetric stretching frequency. As expected, the frequencies of the two bending modes decrease going down the group. Interestingly, for BH_3, AlH_3, and GaH_3, the value of ν_2 is less than ν_4; however, the ordering of these two modes is reversed for InH_3, TlH_3, and $(E113)H_3$, which means that in-plane bending requires less energy than out of plane bending for the heavier hydrides. Again, the decrease in the in-plane bending frequencies for the heavier trihydrides allows

(71) (a) Schwerdtfeger, P.; Bowmaker, G. A.; Boyd, P. D. W.; Ware, D. C.; Brothers, P. J.; Nielsen, A. J. *Organometallics* **1990**, *9*, 504. (b) Kurbakova, A. P.; Bukalov, S. S.; Leites, L. A.; Golubinskaya, L. M.; Bregadze, V. I. *J. Organomet. Chem.* **1997**, *536*−*537*, 519.

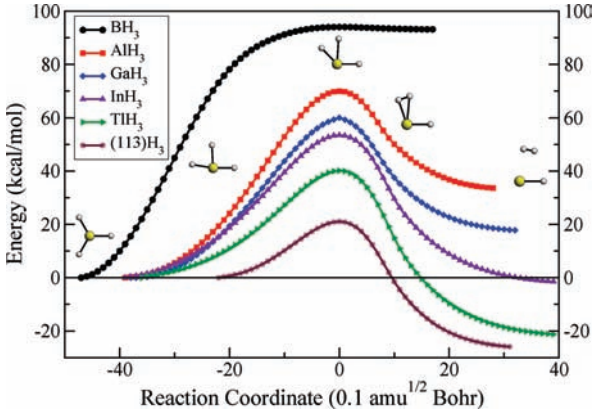

Figure 1. IRC energy profiles for the decomposition path of EH_3 (E = B to E113) from MP2 calculations.

for easier decomposition of these species, as we shall see below, the structures at the transition state all occur in-plane of these molecules.

Thermodynamic Stability. The thermodynamic analyses for the gas-phase decomposition of EH_3 and $TlMe_3$ at standard conditions (298 K and 1 atm) are given in Table 4. The dissociation of EH_3 becomes more exothermic and thermodynamically favorable going down the group as pointed out before.[7] BH_3, AlH_3, and GaH_3 are all thermodynamically stable at 298 K. The decomposition of InH_3 is borderline, with small positive value for ΔH, and a small negative one for ΔG at the coupled-cluster level of theory. TlH_3 and $(E113)H_3$ are both thermodynamically unstable. Schwerdtfeger et al.[7] previously calculated that the MP2 ΔE + zero-point vibrational correction values for the decomposition of BH_3 to TlH_3 were 89.1, 27.8, 18.8, 4.3, and −11.6 kcal/mol, respectively, in good agreement with our MP2 results. Seth et al.[43] also calculated the decomposition energy of $(E113)H_3$ to be −30.3 kcal/mol from CCSD(T) calculations with a spin−orbit averaged pseudopotential, in reasonable agreement with our Dirac-MP2 calculations. Concerning the DFT results, the stabilities of all of the trihydrides are underestimated relative to the MP2 and CCSD(T) calculations. Interestingly, all of our calculations predict that InH_3 is thermodynamically unstable. Furthermore, our MP2 and CCSD(T) calculations predict that the decomposition of $TlMe_3$ is thermodynamically favorable. Concerning our relativistic Dirac-MP2 results, we find that spin−orbit effects significantly lower the energy of decomposition of $(E113)H_3$ by 16 kcal/mol compared to our scalar relativistic pseudopotential MP2 calculations. This is in accordance with the energetic spin−orbit stabilization and resulting chemical inertness of the $p_{1/2}$ shell of the heavier hydrides. The thermodynamic stability of the group 13 hydrides has been discussed already in great detail before,[7] and we therefore turn now to a more detailed analysis of their kinetic stability.

Kinetic Stability. The decomposition paths from our IRC calculations at the MP2 level of theory are shown in Figure 1 for all EH_3 molecules, and the structural parameters for the corresponding transition states are given in Table 5. Here we used the atomic labeling schemes as given in Figure 2 for both EH_3 and $TlMe_3$. All structures

Table 3. Calculated Harmonic (H) and Anharmonic (AH) Vibrational Frequencies (in cm^{-1}) for the Group 13 Hydrides EH_3(E = B to E113) at the MP2 Level of Theory[a]

molecule	method	$\nu_1(A_1')$ sym str	$\nu_2(A_2'')$ out of plane	$\nu_3(E')$ asym str	$\nu_4(E')$ bend
BH_3	H-MP2	2634(0)	1179(90)	2767(129)	1246(16)
	AH-MP2	2585	1167	2719	1234
	MI-IR (Ar)[12]		1125	2808	1604
	IR (gas)[13]		1140.7		
AlH_3	H-MP2	1979(0)	746(380)	1975(274)	787(240)
	AH-MP2	1964	743	1952	785
	MI-IR (Ar)[14]		697.6	1882.7	783.5
	MI-IR (H_2/Ar)[15]		697.8	1882.8	783.4
	MI-IR (Ar)[19]		697.7	1882.9	783.6
GaH_3	H-MP2	2081(0)	760(198)	2074(258)	789(155)
	AH-MP2	2061	758	2046	788
	MI-IR (H_2)[18]		719.2	1928.7	758.0
	MI-IR (Ar)[19]		717.4	1923.2	758.7
InH_3	H-MP2	1921(0)	655(224)	1905(308)	627(187)
	AH-MP2	1903	653	1880	625
	MI-IR (Ar)[19]		613.2	1754.5	607.8
	MI-IR (H_2)[21]		615.3	1760.9	609.1
TlH_3	H-MP2	1954(0)	705(94)	1924(343)	503(143)
	AH-MP2	1932	701	1895	497
	MI-IR (H_2)[22]			1748.4	
$(E113)H_3$	H-MP2[b]	2290(3)	1001(2)	1664(686)/2197(186)	565(26)/626(37)
	AH-MP2[b]	2236	983	1619/2171	482/621

[a] The calculated IR intensities (in km/mol) are given within parentheses after the harmonic frequency. All anharmonic frequencies include anharmonic corrections from MP2 calculations. Unless otherwise stated, the data given are from this study. [b] T-shaped C_{2v} structure.

Table 4. Gas Phase Decomposition Energies for the Group 13 Hydrides ($EH_3 \rightarrow EH + H_2$) and for $TlMe_3$[a]

		$EH_3 \rightarrow EH + H_2$					
theory	compound	$E^{\dagger}$	ΔE	ΔE + ZPE	ΔH	ΔG	ΔS
MP2	BH_3	94.0	94.2	87.3	89.0	80.9	27.2
	AlH_3	70.0	34.4	31.5	33.1	25.2	26.4
	GaH_3	60.0	18.6	15.2	16.8	8.8	26.8
	InH_3	53.5	−0.7	−3.0	−1.5	−9.3	26.1
	TlH_3	40.2	−20.7	−22.9	−21.5	−29.2	25.8
	$TlMe_3$	56.3	−25.1	−23.7	−24.4	−30.3	19.9
	$(E113)H_3$	21.1	−21.2	−24.6	−23.1	−29.9	23.0
CCSD(T)	BH_3	88.4	88.1	81.2	82.9	74.8	27.2
	AlH_3	65.3	31.9	29.0	30.6	22.8	26.4
	GaH_3	57.7	17.6	14.3	15.9	8.0	26.7
	InH_3	52.6	1.7	−0.5	1.1	−6.7	26.0
	TlH_3	41.3	−16.6	−18.6	−17.2	−24.9	25.8
	$TlMe_3$[c]	57.1	−24.4	−23.1	−23.7	−29.7	19.9
	$(E113)H_3$	21.6	−22.9	−25.9	−24.4	−31.6	24.2
B3LYP	BH_3	[b]	90.8	84.0	85.7	77.6	27.2
	AlH_3	63.6	28.8	25.9	27.5	19.6	26.5
	GaH_3	55.5	13.0	9.9	11.5	3.6	26.7
	InH_3	51.1	−2.1	−4.0	−2.5	−10.3	26.0
	TlH_3	40.4	−19.9	−21.6	−20.2	−27.8	25.7
	$(E113)H_3$	19.0	−33.1	−34.0	−33.1	−39.6	21.6
PW91	BH_3	[b]	93.0	86.3	88.1	80.0	27.2
	AlH_3	56.1	29.8	27.0	28.6	20.7	26.4
	GaH_3	49.7	15.8	12.8	14.4	6.4	26.7
	InH_3	45.9	1.0	−0.9	0.6	−7.1	25.9
	TlH_3	35.9	−15.8	−17.4	−16.0	−23.7	25.6
	$(E113)H_3$	16.7	−26.7	−27.6	−26.7	−33.3	22.1
Dirac-MP2	TlH_3	41.0	−17.1				
	$(E113)H_3$	15.0	−37.0				

[a] All energies in kcal/mol with ΔS in cal/(mol K) at standard conditions. [b] No stable transition state could be located. [c] The ZPE, enthalpy, and Gibbs free energy corrections were added from the MP2 vibrational analysis.

of the transition state are planar but breaking C_{2v} symmetry and only maintaining C_s symmetry along the reaction path. To check for the possibility of a non-planar transition state structure, we manually adjusted the geometry of each transition state structure by rotating leaving hydrogen molecule ($H_{(2)}-H_{(3)}$) by 30 and 90 degrees out of plane. The structure with H_2 rotated out by 30 degrees optimized back to the planar structure. The one rotated by 90 degrees optimized into a second-order saddle point with an additional imaginary frequency for rotating the leaving hydrogen molecule out of the perpendicular plane. For $TlMe_3$, we also obtain an almost planar TlC_3 arrangement with the $C_{(1)}-Tl-C_{(2)}-C_{(3)}$ dihedral angle (δ) of 178.9°.

Table 5. Structural Parameters for the EH_3 Transition States (TS) and van der Waals Complexes (VDW)[a]

structure	M	method	E−H_1	E−H_2	E−H_3	H_2−H_3	H_1−E−H_2	H_1−E−H_3
TS	B	MP2	1.216	2.003	1.773	0.768	73.2	95.6
		CCSD(T)	1.222	1.962	1.718	0.780	73.4	96.7
	Al	MP2	1.560	1.782	1.571	1.378	86.7	134.7
		CCSD(T)	1.572	1.816	1.583	1.430	83.3	132.5
	Ga	MP2	1.512	1.769	1.521	1.442	83.2	134.5
		CCSD(T)	1.537	1.828	1.544	1.490	80.6	132.2
	In	MP2	1.661	1.942	1.666	1.473	93.5	140.9
		CCSD(T)	1.694	2.021	1.698	1.510	90.8	137.7
	Tl	MP2	1.659	1.987	1.657	1.495	98.7	146.1
		CCSD(T)	1.694	2.070	1.688	1.523	97.8	144.2
	E113	MP2	1.689	1.997	1.683	1.441	102.5	147.6
		CCSD(T)	1.708	2.054	1.695	1.461	103.2	147.8
VDW	B	MP2	1.217	2.739	2.542	0.741	70.1	85.7
	Al	MP2	1.645	2.707	2.786	0.743	62.0	77.5
	Ga	MP2	1.645	2.768	2.857	0.742	64.2	79.2
	In	MP2	1.821	2.933	3.083	0.742	62.0	75.8
	Tl	MP2	1.874	2.905	3.070	0.742	63.7	77.6
	E113	MP2	1.905	2.577	2.635	0.747	71.7	88.1

[a] All bond lengths in Å, and all angles in degrees. All structures are planar.

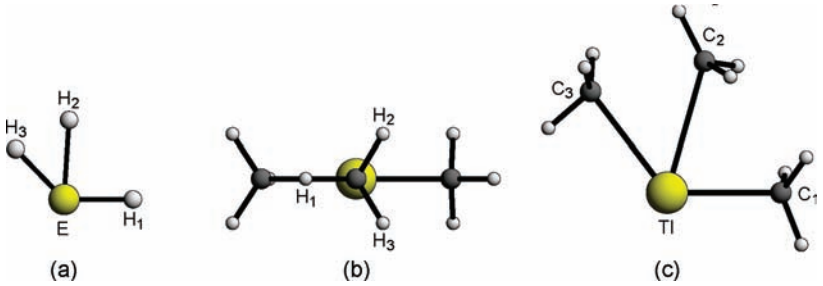

Figure 2. Atomic labeling scheme used for the EH_3 (E = B to E113) transition state (a), $TlMe_3$ minimum (b) and transition state (c).

We observe some interesting trends in the transition state structures of the EH_3 molecules, which are connected to the Hammond−Leffler postulate for early/late transition states in chemical reactions.[72,73] The overall mechanism for the decomposition of EH_3 involves the bending of $H_{(2)}$ and $H_{(3)}$ toward each other with a concomitant weakening of the E−$H_{(2)}$ and E−$H_{(3)}$ bonds. For the two hydrogens which will form a bond along the decomposition pathway, the E−$H_{(2)}$ and E−$H_{(3)}$ distances decrease dramatically from BH_3 to AlH_3 indicating a change from a late transition state in BH_3 to an early transition state in AlH_3. In fact, for the E−$H_{(3)}$ bond distance we observe the trend $BH_3 \gg AlH_3 > GaH_3$. From InH_3 to $(E113)H_3$ the increasing atomic radius becomes apparent, and the E−H_3 bond distances are about the same for the heavier hydrides, but still smaller compared to BH_3. This trend is further reinforced by the difference between the E−$H_{(1)}$ bond length in the transition state and the corresponding equilibrium E−H bond length (see Table 1), that is, the B−$H_{(1)}$ bond distance is close to that calculated for the dimer BH, while for the heavier hydrides the E−$H_{(1)}$ distance is closer to that of EH_3. We note that the overall trends calculated for the decomposition process are similar to that of the group 14 hydrides discussed by Merino et al.[46]

For $TlMe_3$ we obtain the following MP2 bond distances (in Å) and angles (in degrees) for the transition state structure: Tl−$C_{(1)}$ 2.277, Tl−$C_{(2)}$ 2.691, Tl−$C_{(3)}$ 2.457, $C_{(1)}$−$C_{(2)}$ 2.974, $C_{(1)}$−$C_{(3)}$ 4.224, $C_{(2)}$−$C_{(3)}$ 2.317, $C_{(1)}$−Tl−$C_{(2)}$ 73.0, $C_{(2)}$−Tl−$C_{(3)}$ 53.3, $C_{(1)}$−Tl−$C_{(2)}$−$C_{(3)}$ 178.9. We find that the mechanism for the decomposition of $TlMe_3$ is quite similar to those of the EH_3 molecules in that two of the methyl groups ($C_{(2)}$ and $C_{(3)}$) rearrange such that they can form a carbon−carbon bond. This rearrangement is accompanied by a weakening of all three Tl−C bonds and in line with an early transition state.

The activation energies ($E^{\dagger}$) at different levels of theory are listed in Table 4. They decrease toward the heavier element hydrides as can be clearly seen in Figure 1. As mentioned before, the decomposition of InH_3 to $(E113)H_3$ are energetically favored and the IRC curves are typical for an early transition state. Hence the curves shown in Figure 1 are a nice example of the Bell−Evans−Polanyi principle[74] where exothermic reactions are in accordance with an early transition state (see ref 75 for a detailed discussion). Interestingly, the recombination of BH and H_2 to BH_3 is almost barrierless, indicating that the BH molecule is highly unstable in the presence of hydrogen. The density functionals used in this study cannot properly describe weakly interacting systems, and we were unable to locate a stable transition state for the decomposition of BH_3, that is, all attempts to find

(72) Hammond, G. S. *J. Am. Chem. Soc.* **1955**, *77*, 334.
(73) Leffler, J. E. *Science* **1952**, *117*, 340.
(74) (a) Bell, R. P. *Proc. Roy. Soc. London A* **1936**, *154*, 414. (b) Evans, M. G.; Polanyi, M. *Trans. Faraday Soc.* **1938**, *34*, 11.
(75) Anglada, J. M.; Besalú, E.; Bofill, J. M.; Crehuet, R. *J. Comput. Chem.* **1999**, *20*, 1112.

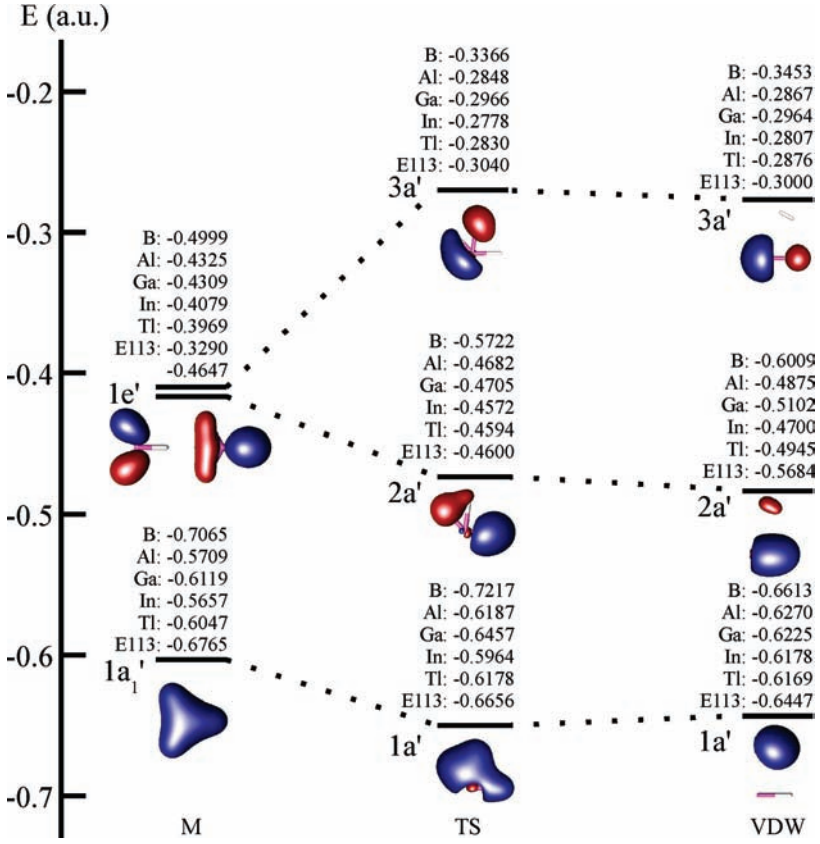

Figure 3. Orbital energies for the minimum (M) of D_{3h} symmetry, transition state (TS) and van der Waals (VDW) structures of C_s symmetry for all EH_3 (E = B to E113) compounds.

a van der Waals interaction between BH and H_2 minimized to the structure of BH_3. Moreover, in all cases, the activation energies obtained from DFT calculations (not listed here) are lower than those from CCSD(T) theory, in some cases by more than 4 kcal/mol. In accordance, the reaction energies from DFT are also lower than those from CCSD(T), and this difference becomes greater going down the group 13 element hydrides. We also find that the activation energies are lowered by roughly 4−6 kcal/mol. We calculate an activation barrier of 56 kcal/mol from our MP2 calculations for the decomposition of $TlMe_3$. This value is similar to the activation energy for GaH_3. Hence, the stability of $TlMe_3$ is due to kinetic effects.

Orbital Analysis. The bonding picture of the Group 13 hydrides is rather complex, which can easily lead to the misinterpretation of the inert pair effect for these systems. Figure 3 depicts the evolution of the main occupied orbitals involved in the decomposition of the EH_3 compounds, that is, from the EH_3 minimum to the transition state, and finally the van der Waals product. Because of symmetry breaking from D_{3h} to C_{2v} for the minimum structure of $(E113)H_3$, the 1e′ orbitals split into $1b_2$ and $1a_1$, and two orbital energies are listed for this case. For the EH_3 molecules the e′ orbitals involve σ-type bonding among two of the valence p-orbitals of the group 13 element and the three hydrogen 1s orbitals, while the a_1' orbital reflects the totally bonding interaction among the 1s orbitals of hydrogen and the valence s-shell of the group 13 element. While the orbital energies increase monotonically for the e′-HOMO, reflecting weaker 1s(H)-*n*p(E) bonding going down the group 13 of elements, the a_1' orbital energies exhibit a typical zigzag behavior pointed out and discussed in terms of the inert-pair effect by many authors.[7,8,36−38] Here we only note that this alternating trend is not in-line with the valence-*n*s ionization potentials of the group 13 atoms.[39] The exception to this trend is the a_1' orbital for $(E113)H_3$ which is rather low because of relativistic effects. We note that the NBO charges on the group 13 elements also fluctuate in the familiar zigzag pattern going down the group, see Table 6.

On the product side, the decomposition of EH_3 leads to the formation of a van der Waals complex with H_2 weakly bound to EH and to the formation of a σ bond of the leaving hydrogen molecule ($1a_1' \rightarrow 1a'$). In this van der Waals complex, the H_2 is slightly polarized by EH resulting in negligible charge transfer, that is, the NBO charges for hydrogen in H_2 are almost zero which is of no surprise. In the canonical picture (Hartree−Fock or Kohn−Sham) the bonding situation in this van der Waals complex is quite different of what one expects. If we assume that the group 13 element *n*s orbital is inert (no sp hybridization), the HOMO would mainly consist of a σ-bonding orbital between E(p_σ) and H(1s). This is indeed the case for BH. However, as shown in Table 6 the charge of the group 13 element increases substantially from B to all the other group 13 elements, thus leading to a charge depletion in the valence *n*p orbitals. This goes along with an increased valence *n*s admixture in the highest occupied molecular orbital (HOMO) despite the increasing *n*s population, thus contradicting the inert pair effect. Here we see the formation of a σ-bond between the group 13 element and hydrogen in the EH molecule ($1e' \rightarrow 2a'$), as well as a σ^*

Table 6. NBO Charges q and Metal Valence s- and p-Populations (n_s and n_p) of the Stationary Points of the EH_3 Compounds[a]

		B	Al	Ga	In	Tl	E113
Min	q(M)	0.42	1.33	1.06	1.19	0.96	0.54
	n_s(M)	0.95	0.81	0.92	0.89	1.04	1.42
	n_p(M)	1.63	0.85	1.02	0.94	1.05	1.21
TS	q(M)	0.30	0.81	0.62	0.80	0.66	0.40
	n_s(M)	1.72	1.04	1.17	1.11	1.30	1.63
	n_p(M)	1.97	1.13	1.20	1.10	1.10	1.13
	q(H_1)	−0.32	−0.34	−0.24	−0.31	−0.24	−0.15
	q(H_2)	0	−0.33	−0.29	−0.37	−0.37	−0.30
	q(H_3)	0.02	−0.14	−0.09	−0.12	−0.05	0.05
VDW	q(M)	0.38	0.65	0.61	0.65	0.64	0.56
	n_s(M)	1.79	1.83	1.85	1.86	1.89	1.93
	n_p(M)	0.82	0.50	0.53	0.49	0.48	0.54
	q(H_1)	−0.38	−0.65	−0.61	−0.65	−0.64	−0.56

[a] Min denotes the minimum, TS the transition state, and VDW the van der Waals complex of the decomposition product. For the VDW complex the charges for H_2 and H_3 are between −0.01 and +0.01. We do not list the values for MH as they are almost identical to MH in the VDW complex.

antibonding HOMO between E and H (1e′→3a′) as shown on the right-hand side in Figure 3. However, the NBO analysis tries to identify Lewis structures and leads to a more localized picture. Here the contributions from the valence s and p orbitals of the group 13 element to the E−H bond in the VDW product are: 15% s and 85% p (B), 11% s and 88% p (Al), 10% s and 89% p (Ga), 9% s and 90% p (In), 7% s and 92% p (Tl), and 5% s and 95% p (E113). This rather indicates diminishing s-character for the heavier elements and is in-line with the inert-pair effect. Hence, one has to be careful what bonding picture is applied.

The driving force for the decomposition reaction is the formation of a stable σ bond for H_2. However, a significant portion of the activation energy comes from the formation of the antibonding 3a′ orbital, and the energy difference to the e′ orbital of EH_3 decreases going down the group (0.163, 0.148, 0.134, 0.130, 0.114, 0.025 au for B, Al, Ga, In, Tl, E113, respectively). The NBO charges on the group 13 elements decrease from the educt to the transition state and further to the product, reflecting already partial reduction of the group 13 atoms in the transition state. The decrease toward the transition state in charge varies from 0.12 for E113 to as much as 0.52 for Al. The charge transfer of typically 0.2−0.3 electrons comes primarily from the $H_{(2)}$ and $H_{(3)}$ atoms in the transition state structures and going into the valence s and p orbitals of the group 13 element as one expects. The only exception to this trend is BH_3, as the transition state is very late in the reaction profile and is almost entirely product-like. Moreover, the transfer of electron density in the transition state becomes smaller going down the group 13 elements as the transition state becomes more educt-like, with E113 even showing a decrease in the valence p occupation toward the transition state. Going from the transition state to the van der Waals product, the charge of the group 13 atoms decreases by a further 0.3−0.5 electrons, with the exception being E113, whose charge actually increases by 0.14 because of relativistic effects. Interestingly, the valence p populations of all of the group 13 atoms decrease along the reaction path going to the van der Waals product. We also see that the d orbitals become slightly more involved in the bonding going down the group, with $(E113)H_3$ having an overall d occupancy of $n_d = 9.84$ electrons in the minimum structure, while for the other group 13 hydrides d-participation can be neglected (e.g., $n_d = 9.96$ for TlH_3 and 9.98 for TlH_3). Seth et al.[43] predicted that the reasoning behind a T-shaped minimum for $(E113)H_3$ could be due to the mixing of the 6d and 7s electrons, and that E113 behaves like a (very) late transition metal.

For the sake of completeness, we give the NBO charges for the organo-thallium compounds. For TlMe we have q(Tl) = 0.70 and q(C) = −1.25, and for $TlMe_3$ q(Tl) = 1.37 and q(C) = −1.03. For the transition state we get q(Tl) = 0.63, $q(C_{(1)})$ = −1.05, $q(C_{(2)})$ = −0.62, and $q(C_{(3)})$ = −0.58. In ethane we have q(C) = −0.50. The situation for $TlMe_3$ is similar to that of TlH_3, but there is a significant decrease in charge on the Tl atom with a concomitant increase in charge on $C_{(2)}$ and $C_{(3)}$ for the transition state while the charge of $C_{(1)}$ does not change significantly going from the minimum to the transition state.

Conclusions

Wave function and density functional based methods were used to investigate in detail the gas phase decomposition pathways of the group 13 hydrides, EH_3, (E = B to E113). For the hydrides of Tl and E113, we also performed Dirac-MP2 calculations to include important spin−orbit effects. All of the transition state structures are found to be planar, and the IRC analyses revealed that the decomposition process is described by two hydrogen atoms bending toward each other to form a H−H bond, with a concomitant weakening of two E−H bonds and the breaking of C_{2v} symmetry. All of our calculations showed that the activation energy decreases significantly going from B to E113, with the activation barrier being only 21 kcal/mol for $(E113)H_3$ from our MP2 and CCSD(T) calculations. The activation energy for BH_3 is close to its decomposition energy, that is, the formation of BH_3 from BH and H_2 is almost barrierless. The in-plane bending modes for the EH_3 compounds decrease going down the group, so much that the D_{3h} structure becomes a second-order saddle point for $(E113)H_3$. Spin−orbit coupling also plays an important role in lowering the activation barrier by 6 kcal/mol for (E113)H. We also provided a detailed orbital analysis to rationalize our results. We finally mention that at low temperatures a bimolecular decomposition process $2EH_3 \rightarrow E_2H_6 \rightarrow E_2H_4 + H_2 \rightarrow E_2H_2 + 2H_2$ should be considered as well which could have lower barriers. However, these calculations are far more computer time intensive and will be the subject of our future investigations.

Acknowledgment. Support from the Marsden Fund (Wellington) is gratefully acknowledged. K.K. thanks the European Science Foundation for financial support. We are grateful to K. A. Peterson (Washington State University) for the valence basis sets prior to publication.